

## Comparación de Herramientas de Simulación CFD en el Estudio del Efecto Vórtice sobre Punta de Aspa para Rotor Eólico

### Comparison of CFD Simulation Tools in the Study of Vortex Effect on Wind Rotor Blade Tip

Tatiana Ortegon Sarmiento <sup>1</sup>.; William Gomez Rivera<sup>2</sup>.; Hernan Ceron <sup>3</sup>

<sup>1</sup> Research assistant, Universidad Militar Nueva Granada. taxipiorsa@hotmail.com

<sup>2</sup> Professor, Universidad Militar Nueva Granada. william.gomezr@unimilitar.edu.co

<sup>3</sup> Professor, Universidade de São Paulo. hernan@sc.usp.br

#### Resumen

Actualmente existen diversas herramientas para la simulación del comportamiento dinámico de los fluidos, muchas de las cuales son comerciales o de código abierto. Ansys y OpenFOAM (Open Field Operation and Manipulation) son algunas de ellas, sin embargo, existen marcadas diferencias durante las etapas de pre-procesamiento, procesamiento y post-procesamiento. A fin de analizar las ventajas y desventajas que estos dos códigos ofrecen, así como las diferencias en resultados, en este trabajo se analizó específicamente el efecto de vórtice que se crea sobre la punta de un aspa para rotor eólico. Para el caso específico se realizó un análisis 3D de un aspa con cuerda variable y perfiles NREL-S811, NREL-S809 y NREL-S810 (desde la raíz hasta la punta). El análisis incluye el uso de una punta base (sin modificación), y una tipo Tip-Tank, y la comparación de los coeficientes aerodinámicos ( $C_L$ ,  $C_D$  y  $C_M$ ) y los vórtices generados sobre cada una de estas. Para el estudio se utilizó el modelo de turbulencia k-epsilon, y Reynolds  $Re=1.44 \times 10^5$ . Se evidenció que tanto en Ansys como en OpenFOAM, la intensidad del vórtice obtenido varía dependiendo de múltiples factores como tamaño del elemento, así como del modelo de turbulencia. Con los resultados obtenidos se evidenció para el caso de OpenFOAM que la punta Tip Tank presentó un coeficiente de sustentación mayor en un 22.9% respecto a la punta base, y un coeficiente de arrastre mayor en un 3.74%, mientras que para el caso de Ansys, la

punta Tip Tank presentó un coeficiente de sustentación mayor en un 0.25% respecto a la punta base, y un coeficiente de arrastre mayor en un 3.14%. La utilización de OpenFOAM requiere de un acertado conocimiento de las variables de flujo y de la aerodinámica del caso bajo estudio, toda vez que al tratarse de un código basado en programación C++, el usuario puede incurrir en errores que no son evidentes y afectan sensiblemente el comportamiento teórico del modelo aerodinámico. Por el contrario, ANSYS es más amigable en cuanto al análisis, sin embargo, es poco flexible en la modificación de las variables base.

*Palabras clave:* ansys, energía eólica, openfoam, vórtice.

#### Abstract

At present there are several tools for simulating the dynamic behavior of fluids, many of these are commercial or open source. Ansys and OpenFOAM (Open Field Operation and Manipulation) are some of them, however, there are marked differences during the pre-processing, processing, and post-processing stages. In order to analyze the advantages and disadvantages that these two codes offer, as well as the differences in results, in this paper we specifically analyzed the vortex effect that is created on the tip of a wind rotor blade. For the specific case, a 3D analysis of a blade with variable chord and profiles NREL-S811, NREL-S809 y NREL-S810 (from root to

tip) was performed. The analysis includes the use of a base tip (without modification) and a Tip Tank type, and the comparison of the aerodynamic coefficients ( $C_L$ ,  $C_D$  and  $C_M$ ) and the vortices generated on each of these. For the study we used the k-epsilon turbulence model and Reynolds  $Re=1.44 \times 10^{-5}$ . We evidenced that in both Ansys and OpenFOAM, the intensity of the vortex obtained varies depending on multiple factors such as size of the element, as well as the turbulence model. With the results obtained, it was evident for the case of OpenFOAM that the Tip Tank presented a lift coefficient higher by 22.9% with respect to the base tip, and a drag coefficient greater by 3.74%, while in the case of

Ansys, the tip tank device had a lift coefficient higher by 0.25% with respect to the base tip, and a greater drag coefficient by 3.14%. The use of OpenFOAM requires an accurate knowledge of the flow variables and the aerodynamics of the case under study, since being a code based on C++ programming, the user can commit errors that are not evident and significantly affect the theoretical behavior of the aerodynamic model. In contrast, Ansys is more user-friendly in terms of analysis, however, it is less flexible in the modification of the base variables.

*Keywords:* ansys, wind power, openfoam, vortex.

## 1.-Introduction

Over the years, wind energy has gained great strength as an alternative source to the use of fossil fuels to obtain energy in a cleaner and more efficient way. Many people are currently working on the development of new aerodynamic designs of wind turbines to improve the aerodynamics of these to achieve the highest efficiency possible and maximize the energy conversion capacity at the lowest cost (Ali *et al.*, 2015). The aerodynamic efficiency of wind turbines depends on the aerodynamic design of the blades, their dimensions, construction material and the angle of attack (Raj *et al.*, 2016). With a good aerodynamic design of the blades we can obtain improvements in the efficiency of the turbines, however, there are aerodynamic losses that affect the extraction capacity and energy generation of these, such is the case of the losses related to the vortices generated at the tips of the blades due to the difference in pressure between the intrados and the extrados (Ali *et al.*, 2015), this type of loss is caused by the induced drag, associated with the lift force and with its dependence on the angle

of attack (Sadraey, 2009). Losses are also caused by the skin friction drag, this is the aerodynamic resistance caused by the contact of a fluid with the surface of a body, in this case the contact with the surface of the blades (UVU aviation, 2013). The skin friction drag depends on the viscosity of the air and occurs in the boundary layer when the airflow around an object is altered by surface imperfections. Rough surfaces speed up the transition from laminar to turbulent flow of the boundary layer airflow (UVU aviation, 2013; SKYbrary, 2017).

The vortices generated at the wind rotor blade tips have been studied in many opportunities with most of these investigations focused on computational fluid dynamics (CFD). Simulation tools such as Ansys and OpenFOAM allow the analysis of fluid behavior and the solution of problems related to the dynamics of solids and electromagnetism (ESI Group, 2011).

OpenFOAM is an open source software that allows to solve Computational Fluid Dynamics and Continuum Mechanics applications (Rivera and Furlinger, 2011). This tool uses the Finite Volume Method for the solution of

partial differential equations using the laws of conservation (mass, momentum and energy) in the form of integral equations (Mara *et al.*, 2014). OpenFOAM has different libraries that provide efficiency in the solution of fluid dynamics problems, including mesh, parallelization and various turbulence models for incompressible and compressible flows (Rivera and Furlinger, 2011). In addition to this and considering that the software is a collection of C++ code, it offers flexibility by allowing the user to modify and create their own libraries and solvers, however, it has limited documentation and references (Lysenko *et al.*, 2013).

Ansys, on the other hand, is a high-performance commercial CFD tool that includes different simulation packages, notably CFX. This package is used for the simulation of processes with fluids, or with heat transfer, being of great precision, speed and robustness in the analysis of rotating machinery (ANSYS, Inc., 2018). Like OpenFOAM, Ansys CFX supports the finite volume method (Mara *et al.*, 2014).

In this paper we analyze the aerodynamic performance of two different tip devices of wind turbine blade with variable chord, a tip device without modifications, and one type Tip-Tank, by determining and comparing the lift, drag and moment aerodynamic coefficients ( $C_L$ ,  $C_D$  and  $C_M$ ), as well as the generated vortices, using simulation tools in CFD. The above, with the aim of analyzing the results in both Ansys and OpenFOAM, to understand the advantages and disadvantages offered by these two tools.

This article is organized as follows: Section 2 presents the design of the wind turbine blades, and the simulation of the tip devices. Section 3 presents the results obtained in the

simulations and the analysis of the aerodynamic coefficients and the vortices generated on each of the tips. Finally, in section 4 we present the conclusions.

## 1. Development

For the comparison of the Ansys and OpenFOAM simulation tools, the vortex effect generated on the wind rotor blade tip was chosen as the case study, for which the blade design was carried out, selecting the aerodynamic profiles, followed by their 3D modeling, and their subsequent CFD simulation. Each of these items will be described in detail below.

### 2.1 Wind rotor blade design

The variable chord blades are characterized by a low drag coefficient. These are constructed from different airfoils whose inclination results in torsion and therefore low intensity vortices at the tip (Lysen, 1983). The aerodynamic profiles of the blade were selected so that it is functional and strong. For the selection of the aerodynamic profile of the blade root we considered an airfoil capable of resisting efforts and allowing a good mechanical coupling to the rotor, thus choosing the NREL-S811 airfoil. For the blade body the NREL-S809 airfoil was selected to ensure a high lift and torque coefficient. The airfoil of the blade tip was selected so that there is a certain symmetry between the intrados and the extrados, and that the airfoil allows to incorporate a system of interchangeable tips, thus using the NREL-S810. The distribution of the airfoils along the span of the blade selected for this analysis is shown in Figure 1.

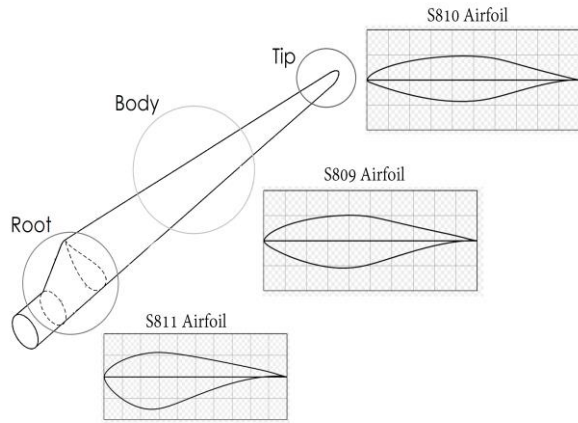


**Figure 1.** Distribution of the aerodynamic profiles on the selected variable chord blade. Source: (Jonkman, 2014; Patente nº US20120269640A1, 2012)

The blade has a length of 0.7m, and a chord of 0.0816m.

Tip Tank devices are characterized by their rounded geometric shape, which allows to take advantage of the generated vortex phenomenon (Sport Aviation, 1971). These devices are used in aviation for fuel storage, however, when they are empty they move the pressure center outwards, reducing the induced drag and increasing the lift at the tips and bending stresses on the wing (Professional Pilots, 2002).

For the selected design, the blade tip corresponds to the final 10% of the total span of the blade, as shown in Figure 2.

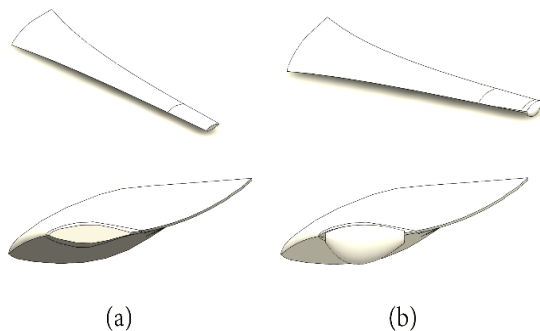


**Figure 2.** (a) Blade with base tip (no modification), (b) blade with Tip Tank device

## 2.2 Simulation

To determine the lift and drag forces and the moment exerted on the blades under study, the simulation was performed using a rectangular domain whose size was established in such a way that it wouldn't affect the results due to parasitic turbulence or losses in the resolution of the velocity contours, thus selecting a size of 24.5 times the chord in each of the axes of the coordinated system.

The airflow velocity was set at 30 m/s with an air density of 1.087 kg/m<sup>3</sup> and a dynamic viscosity of 1.85x10<sup>-5</sup> kg/m\*s, obtaining a Reynolds number equal to Re=1.44x10<sup>5</sup>, as we presented in the Table 1.

**Table 1.** Simulation parameters

	Values
$\rho = \text{Air density (kg/m}^3\text{)}$	1.0879
$T = \text{Temperature (}^\circ\text{C)}$	20
$P_{atm} = \text{Atmospheric pressure (Pa)}$	92600
$V = \text{Wind speed (m/s)}$	30
$Re = \text{Reynolds number}$	144000
$Blade \text{ length (m)}$	0.7
$C_m = \text{Chord (m)}$	0.0816
$\eta = \text{Dynamic viscosity (kg/m}^*\text{s)}$	1.85x10 <sup>-5</sup>
$S = \text{Projected blade area (m}^2\text{)}$	0.03822
$Ma = \text{Mach number}$	0.087

The blades were simulated over a series of angles of attack  $\alpha$  from -10° to 25° with increments of 1°, for this, the blade was left in its initial position varying the direction of the fluid, as shown in Figure 3.

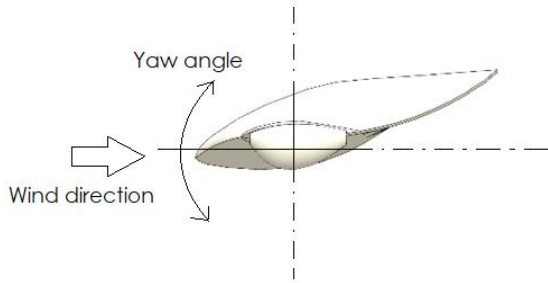


**Figure 3.** Yaw angle setting. The position is shown for  $\alpha = 0^\circ$

The steady-state solver for incompressible turbulent flow was selected based on the Mach number obtained  $Ma = 0.087$ .

For the simulation of the different tip devices it is necessary to build a mesh, for which we used the software package ANSYS ICEM CFD to generate it, and then to use the mesh in openFOAM we imported it into the open source software using the external and open source software Salome Meca together with the script developed by Nicolas Edh (Edh, 2017). For the meshes made, a maximum element size of 0.1 m for the whole domain and a maximum element size of 0.001 m for the blade were defined. In addition, and to refine the mesh around the blade for a better analysis of the behavior of the wake or turbulence, a subdomain was created with a maximum element size of 0.01m. In Figure 4 the domain and the subdomain mesh are presented. The height, length and width of the domain correspond to 24.5 times the chord of airfoil.

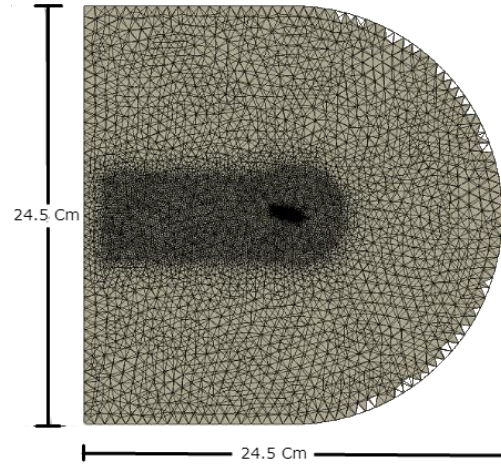


**Figure 4.** Meshed domain of tip devices

For the simulations we used the k-epsilon ( $k-\epsilon$ ) turbulence model, which is one of the most used in computational fluid dynamics due to its capacity to model recirculation flows (Lopez and Muñoz, 2004).

**Table 2.** k-epsilon turbulence model configuration

	Values
$I = \text{Turbulence intensity}$	0.0362528
$k \text{ (m}^2/\text{s}^2)$	1.77426
$\epsilon \text{ (m}^2/\text{s}^3)$	67.8547886

Table 2 presents the configuration parameters of this model, these were calculated using equations (1), (2) and (3).

$$I = 0.16Re^{-1/8} \quad (1)$$

$$k = \frac{3}{2}(V * I)^2 \quad (2)$$

$$\epsilon = \frac{0.164k^{1.5}}{0.07Cm} \quad (3)$$

## 2. Results

The vortices generated at the wind rotor blade tips were identified by creating velocity contour planes located 0.05m from the first chord quarter of the blade. In Figure 5 the

vortices produced on the different tips are displayed, showing that in both Ansys and OpenFOAM the Tip Tank device has a larger vortex diameter than the base tip.

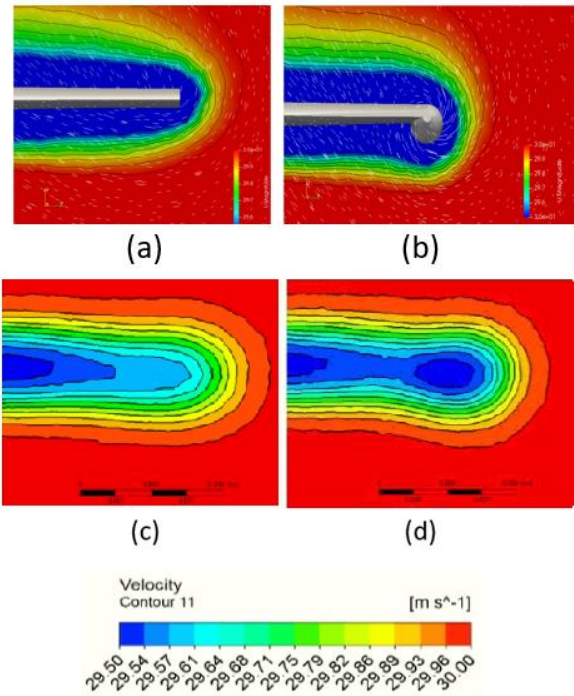


**Figure 5.** Vortices generated in tip devices (a) base tip in OpenFOAM (b) Tip Tank in OpenFOAM (c) base tip in Ansys (d) Tip Tank in Ansys

The Table 3 shows the diameters of the vortices generated on the different analyzed tip devices.

**Table 3.** Vortices generated on the different analyzed tip devices

	Vortex diameter OpenFOAM (m)	Vortex diameter Ansys (m)
Base Tip	0.0156	0.010
Tip Tank	0.0234	0.020

The aerodynamic coefficients of lift  $C_L$  and drag  $C_D$  were obtained from the forces generated on the blade surface in the X and Y ( $F_x$ ,  $F_y$ ) direction for each angle of attack  $\alpha$ . From these forces the drag  $F_D$  and lift  $F_L$

forces were obtained respectively, as shown in Figure 6.

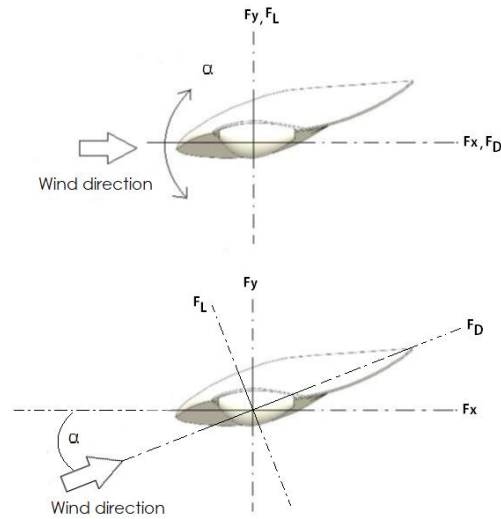


**Figure 6.** Configuration of the forces on the blade surface

Due to the variation of the fluid direction in the simulations, the values of the resulting forces are adjusted so that the drag force is in the fluid direction and the lift force is perpendicular to it, as in Figure 6. To do this, equations (4) and (5) were used to calculate the aerodynamic forces, and equations (6) and (7) (Lysen, 1983) were used to calculate the aerodynamic coefficients, where  $S$  is the projected area of the blade,  $\rho$  the air density, and  $V$  the wind velocity.

$$FL = Fy \cos(\alpha) - Fx \sin(\alpha) \quad (4)$$

$$FD = Fx \cos(\alpha) + Fy \sin(\alpha) \quad (5)$$

$$CL = \frac{FL}{\frac{1}{2} \rho V^2 S} \quad (6)$$

$$CD = \frac{FD}{\frac{1}{2} \rho V^2 S} \quad (7)$$

In Figure 7 the lift coefficients of the different tips analyzed are presented at different angles of attack, showing that increasing this angle increases the lift to a certain point where it stalls. We noted that for the base tip the stall is presented from an angle of attack greater than 21° in the case of openFOAM, while in ansys it was for an angle of attack greater than 19°.

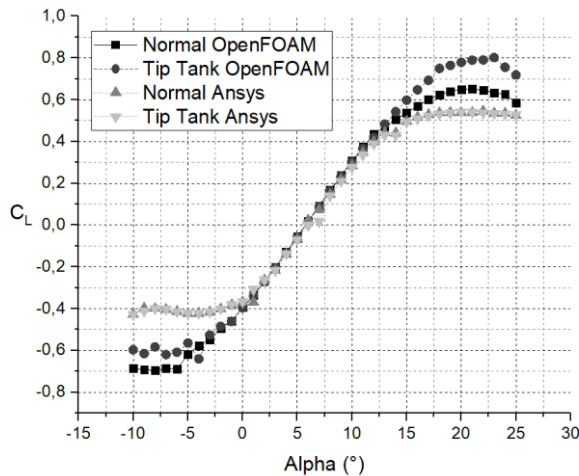


Figure 7. Lift coefficient vs Alpha

For the Tip Tank device, the stall is presented from an angle of attack greater than 23° in the case of openFOAM, while in ansys it was for an angle of attack greater than 20°, as we present on the Table 4.

Table 4. Angle at which devices stall

	Stall angle of attack °	Lift Coefficient
Base Tip OpenFOAM	21	0.65168
Tip Tank OpenFOAM	23	0.80088
Base Tip Ansys	19	0.53957
Tip Tank Ansys	20	0.54091

Likewise, it is evident that the lift coefficient has a linear behavior for the angles of attack between -1° and 13°. It is observed that for the different devices the curve changes the inclination from a certain angle where the growth rate of the lift coefficient begins to decrease (Silva *et al.*, 2014).

The Table 5 shows the lift coefficients obtained for the different tips at angles of attack equal to 10° and 15°. In these angles the highest lift to drag ratio was presented.

Table 5. Lift coefficients for angles of attack  $\alpha=10^\circ$ ,  $15^\circ$

	$C_L$ ( $\alpha=10^\circ$ )	%	$C_L$ ( $\alpha=15^\circ$ )	%
Base Tip OpenFOAM	0.3070	0	0.65168	0
Tip Tank OpenFOAM	0.3012	-1.92	0.80088	11.1
Base Tip Ansys	0.2852	0	0.4981	0
Tip Tank Ansys	0.2759	-3.26	0.4932	-0.984

In the Figure 8 the drag coefficients of the different tip devices obtained with OpenFOAM are presented, showing an increase in the coefficients from the angle of attack  $\alpha = 7^\circ$ .

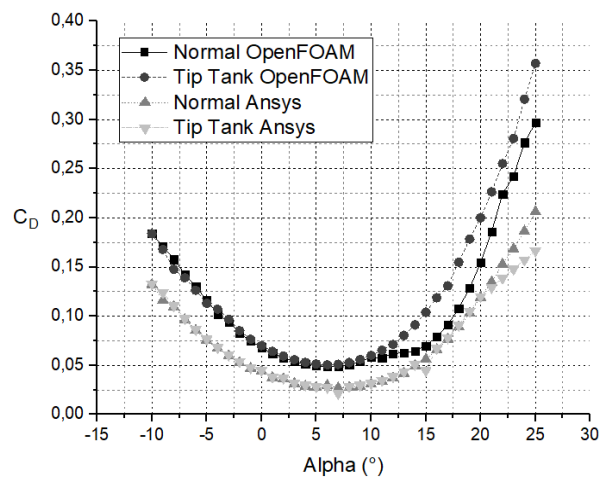


Figure 8. Drag coefficient vs alpha

The Table 6 shows the drag coefficients obtained for the different devices at angles of attack equal to 10° and 15°, showing that for  $\alpha=10^\circ$  in both Ansys and OpenFOAM, the Tip Tank device presented a drag coefficient greater than the base tip.

**Table 6.** Drag coefficients for angles of attack  $\alpha=10^\circ$ ,  $15^\circ$

	$C_D$ ( $\alpha=10^\circ$ )	%	$C_D$ ( $\alpha=15^\circ$ )	%
Base Tip OpenFOAM	0.0581	0	0.65168	0
Tip Tank OpenFOAM	0.0601	3.44	0.80088	22.89
Base Tip Ansys	0.0308	0	0.0562	0
Tip Tank Ansys	0.0317	2.92	0.0446	-20.64

For  $\alpha=15^\circ$ , the Tip Tank had a higher drag coefficient than the base tip, unlike Ansys, where the base tip had a higher drag coefficient than the Tip Tank.

To determine the aerodynamic performance of the tips considered for the analysis, the lift to drag ratio was calculated and plotted based on the angle of attack  $\alpha$ , as shown in Figure 9.

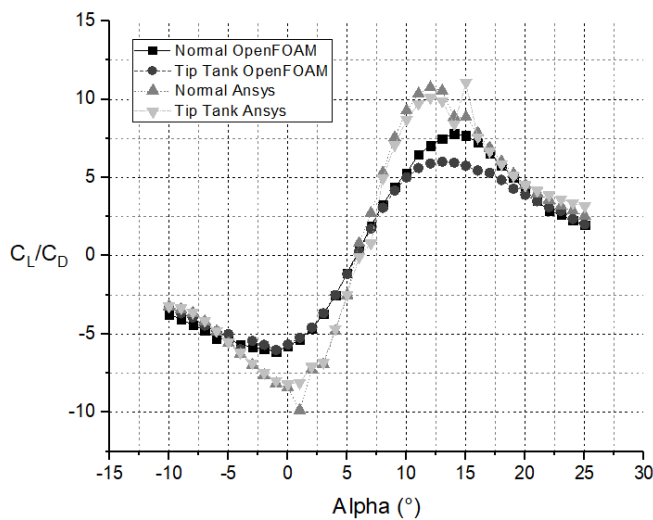


**Figure 9.** Lift to drag ratio vs alpha

The ratio between aerodynamic coefficients  $C_L/C_D$  allows to appreciate the value of the angle of attack in which a better aerodynamic performance is presented.

The Table 7 presents the maximum Lift to Drag Ratio of each tip device and its relation to the base tip.

**Table 7.** Maximum Lift to Drag Ratio of each tip device

	$C_L/C_D$	Angle of Attack	%
Base Tip OpenFOAM	7.794	14°	0
Tip Tank OpenFOAM	6.013	13°	-22.85
Base Tip Ansys	10.749	12°	0
Tip Tank Ansys	10.086	12°	-6.168

We observe that the base tip, the one that has no modification, presented the highest ratio in both Ansys and OpenFOAM.

The graph of the coefficient of moment allows to determine the dynamics of the airfoil on its rotation and the stable positions (Schneider, 2006). As shown in Figure 10, as the angle of attack increases, the coefficient of moment increases slightly to a point where it decreases drastically, being negative.

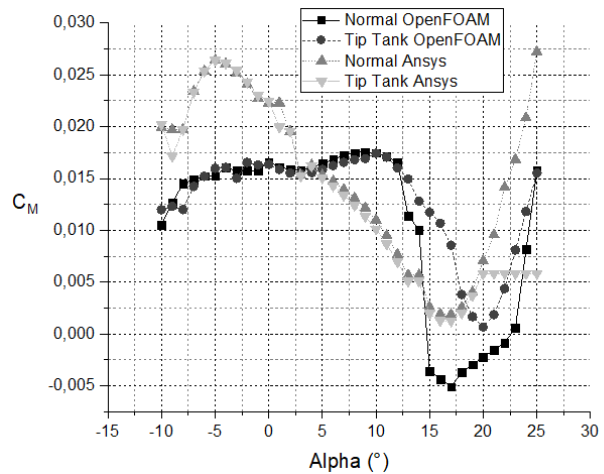


**Figure 10.** Coefficient of moment vs alpha



When the trend line of the different curves of the moment coefficient for each tip device is obtained, it is observed that they have a negative slope. This allows us to conclude that the blade with the different tip devices has a stabilizing behavior (Silva *et al.*, 2014), that is, it is capable of restoring equilibrium to any disturbance that causes a change in the angle of attack (García Rivero, 2010).

### Conclusions

Regarding the obtained coefficients, the studies carried out allow us to conclude that for the case of OpenFOAM the Tip Tank presented a lift coefficient higher by 22.9% with respect to the base tip, and a drag coefficient greater by 3.74%, while in the case of Ansys, the tip tank device had a lift coefficient higher by 0.25% with respect to the base tip, and a greater drag coefficient by 3.14%.

The use of OpenFOAM requires an accurate knowledge of the flow variables and the aerodynamics of the case under study, since being a code based on C++ programming, the user can commit errors that are not evident and significantly affect the theoretical behavior of the aerodynamic model. In contrast, Ansys is more user-friendly in terms of analysis, however, it is less flexible in the modification of the base variables.

### Acknowledgment

The authors would like to thank the Universidad Militar Nueva Granada (UMNG) for the support provided for the development of this work, which was carried out as part of the high-impact project IMP ING 2137 entitled "Development of microturbine to take advantage of the vortex effect in wind

rotor blade tip", 2016-2018, and to the Universidade de São Paulo (USP) for their collaboration and assistance.

### Bibliography

- ESI Group. (2011). *CONSULTING SERVICES WITH OpenFOAM®*. Paris: ESI Group. Obtenido de [https://www.esi-group.com/sites/default/files/resource/brochure\\_flyer/1096/flyer\\_cfd\\_consulting-services\\_openfoam\\_lores.pdf](https://www.esi-group.com/sites/default/files/resource/brochure_flyer/1096/flyer_cfd_consulting-services_openfoam_lores.pdf)
- Ali, A., Chowdhury, H., Loganathan, B., & Alam, F. (2015). An Aerodynamic Study of a Domestic Scale Horizontal Axis Wind Turbine With Varied Tip Configurations. *Procedia Engineering*, 757-762.
- ANSYS, Inc. (2018). *ANSYS CFX*. Obtenido de ANSYS: <http://www.ansys.com/ES/Products/Fluids/ANSYS-CFX>
- Edh, N. (2017). *salomeToOpenFOAM*. Obtenido de <https://github.com/nicolasedh/salomeToOpenFOAM>
- Enevoldsen, P. B., Kristensen, J. J., & Thru, C. (25 de October de 2012). *Patente n° US20120269640A1*. Obtenido de <https://patents.google.com/patent/US20120269640A1/en>
- García Rivero, M. (2010). Estabilidad y Control. En *Diseño de un UAV ligero de propulsión eléctrica para monitorización medioambiental* (págs. 99-118).
- Jonkman, B. (2014). *NREL's S-Series Airfoils*. Estados Unidos: National Renewable energy laboratory.
- Lopez, L., & Muñoz, J. L. (2004). Estudio de la turbulencia a través del modelo k-epsilon, mediante un código tridimensional con esquemas de alto orden. *Información Tecnológica*, 15, 25-28.
- Lysen, E. H. (1983). *Introduction to Wind Energy: Basic and advanced introduction to wind energy with emphasis on water pumping windmills*. CWD Consultancy services wind energy developing countries.
- Lysenko, D. A., Ertesvåg, I. S., & Rian, K. E. (2013). Modeling of turbulent separated



- flows using OpenFOAM. *Computers & Fluids*, 80, 408-422.
- Mara, B. K., Mercado, B. C., Mercado, L. A., Pascual, J. M., & Lopez, N. S. (2014). Development and validation of a CFD model using ANSYS CFX for aerodynamics simulation of Magnus wind rotor blades. *2014 International Conference on Humanoid, Nanotechnology, Information Technology, Communication and Control, Environment and Management (HNICEM)*. Palawan: IEEE.
- Professional Pilots. (2002). *Tip Tanks, pro's and con's*. Obtenido de PPRuNe: <http://www.pprune.org/tech-log/62967-tip-tanks-pro-s-con-s.html>
- Pérez-Amaya, D., Arias-Hernandez, N.A. and Molina-Prado, M.L., Interfaz gráfica para el análisis de las fuerzas de captura en una pinza óptica usando las aproximaciones de Rayleigh y Mie. *Bistua: Revista de la Facultad de Ciencias Básicas*, 14(2), pp. 182-193, 2016. DOI: 10.24054/01204211.v2.n2.2016.2192
- Raj, A., Gurav, R., Sankpal, J., Chavan, D., & Karandikar, P. (2016). Study of output parameters of horizontal axis wind turbines using experimental test setup. *2016 IEEE 1st International Conference on Power Electronics, Intelligent Control and Energy Systems (ICPEICES)* (págs. 1-6). Delhi: IEEE.
- Rivera, O., & Furlinger, K. (2011). Parallel Aspects of OpenFOAM with Large Eddy Simulations. *2011 IEEE International Conference on High Performance Computing and Communications*. Banff, AB, Canada: IEEE.
- Sadraey, M. (2009). Drag Force and Drag Coefficient. En M. Sadraey, *Aircraft Performance Analysis*. VDM Verlag Dr. Müller.
- Schnaidt, M. T. (2006). *Coefficientes Aerodinámicos Cl Cd Cm con un aprofundimiento de Cm al respecto de la estabilidad de vuelo*. Santiago, Chile: Universidad Andres Bello .
- Silva, N., Pedraza, N., Cerón, H., & Téllez, A. (2014). Análisis Aerodinámico Computacional y Experimental para el Ala de un Mini Vehículo Aéreo no Tripulado (VANT). *VIII Congreso Nacional de Engenharia Mecânica*. Uberlândia - MG - Brasil.
- SKYbrary. (27 de July de 2017). *Friction Drag*. Obtenido de SKYbrary: [https://www.skybrary.aero/index.php/Friction\\_DragSport](https://www.skybrary.aero/index.php/Friction_DragSport) Aviation. (1971). *Comparison of Square, Round, and Hoerner Wing Tips*. Sport Aviation.
- UVU aviation. (20 de December de 2013). *Skin Friction Drag*. Obtenido de YouTube: <https://www.youtube.com/watch?v=NjX2jL-LrkI>
- Rojas Reyes NR, Quitian Chila GR, Saldarriaga Agudelo W (2017) Caracterización Magneto-reológica de un Fluido a Base de Desechos Mineros.Ciencia en Desarrollo. 8(2): 61-67
- \*Para citar este artículo: Ortegon Sarmiento T.;Gomez Rivera W.; Ceron H.Comparison of CFD Simulation Tools in the Study of Vortex Effect on Wind Rotor Blade Tip. *Revista Bistua*. 2019 17(1):159-168
- + Autor para el envío de correspondencia y la solicitud de las separatas: Ortegon Sarmiento T. Universidad Militar Nueva Granada. [taxipiorsa@hotmail.com](mailto:taxipiorsa@hotmail.com)

Recibido: Marzo 21 de 2018

Aceptado: Agosto 17 de 2018

